Mutational Analysis of the Active Site and Antibody Epitopes of the Complement-inhibitory Glycoprotein, CD59

By Dale L. Bodian,* Simon J. Davis,‡ B. Paul Morgan,§ and Neil K. Rushmere§

*From the *Laboratory of Molecular Biophysics, Oxford OX1 3QU, United Kingdom; ‡Molecular Sciences Division, Nuffield Department of Clinical Medicine, John Radcliffe Hospital, Headington, Oxford OX3 9DU, United Kingdom; and §Department of Medical Biochemistry, University of Wales College of Medicine, Cardiff CF4 4XN, United Kingdom*

Summary

The Ly-6 superfamily of cell surface molecules includes CD59, a potent regulator of the complement system that protects host cells from the cytolytic action of the membrane attack complex (MAC). Although its mechanism of action is not well understood, CD59 is thought to prevent assembly of the MAC by binding to the C8 and/or C9 proteins of the nascent complex. Here a systematic, structure-based mutational approach has been used to determine the region(s) of CD59 required for its protective activity. Analysis of 16 CD59 mutants with single, highly nonconservative substitutions suggests that CD59 has a single active site that includes Trp-40, Arg-53, and Glu-56 of the glycosylated, membrane-distal face of the disk-like extracellular domain and, possibly, Asp-24 positioned at the edge of the domain. The putative active site includes residues conserved across species, consistent with the lack of strict homologous restriction previously observed in studies of CD59 function. Competition and mutational analyses of the epitopes of eight CD59-blocking and non-blocking monoclonal antibodies confirmed the location of the active site. Additional experiments showed that the expression and function of CD59 are both glycosylation independent.

Complement is a tightly regulated system of proteins that protects a host from infection by invading microorganisms. Complement-mediated immune responses culminate in the assembly of the membrane attack complex (MAC)[1] at the membrane of the foreign organism, forming a pore that leads to osmotic lysis. The cytolytic action of complement is the basis of hyperacute rejection reactions which result in the destruction of xeno- and allografts after transplantation (1). Of the three major membrane-bound proteins that protect host cells from lysis by complement, CD59 (also called membrane inhibitor of reactive lysis [MIRL], protectin, HRF20, and H19), decay-accelerating factor, and membrane cofactor protein, the most potent inhibitor on human endothelial cells is CD59 (2). Deficiency of CD59 is the primary cause of erythrocytic hemolysis observed in patients with paroxysmal nocturnal hemoglobinuria (3, 4). The importance of CD59 is also underscored by the tumor virus Herpesvirus saimiri, which encodes a protein homologous to CD59 apparently as a means of evading the immune system of its host (5, 6).

CD59 appears to function as an inhibitor of complement by binding to C5b-8 or C5b-9 of the assembling MAC, thereby preventing incorporation of the multiple copies of C9 required for complete formation of the osmolytic pore (7, 8). Despite sequence identities as low as 40%, the primate, rat, pig, and sheep homologues are able to function across species barriers, albeit to varying degrees of efficiency (9–11). CD59 may also participate in signal transduction events leading to activation of T cells, thymocytes, and neutrophils (12). Although binding between CD59 and CD2 has been implicated in this mechanism of activation (13, 14), other groups have been unable to detect a specific interaction between these two proteins (15, 16).

CD59 is a widely distributed, glycosylphosphatidylinositol (GPI)-anchored cell surface protein of ~20 kD belonging to the Ly-6 superfamily (Ly-6SF) of cell surface proteins. Ly-6 molecules were first identified in the mouse serologically and, as such, were among the first cell surface molecules identified (reviewed in reference 17). Nevertheless, with the exceptions of CD59 and the urokinase plasminogen activator receptor (reviewed in reference 18), the functions of Ly-6SF molecules are poorly understood. CD59 is the only Ly-6SF protein for which a three-dimensional

[1] *Abbreviations used in this paper:* CHO, Chinese hamster ovary; GPI, glycosylphosphatidylinositol; Ly-6SF, Ly-6 superfamily; MAC, membrane attack complex; MIRL, membrane inhibitor of reactive lysis; NHS, normal human serum; NMR, nuclear magnetic resonance; RT, room temperature.

structure has been determined. Nuclear magnetic resonance (NMR) spectroscopic analyses of human CD59 revealed a single disk-like extracellular domain, formed by single two- and three-stranded β-sheets and a short α-helix, that is attached to the GPI anchor by a seven residue stalk (19, 20). The topology of the extracellular domain is similar to that of snake venom neurotoxins, consistent with the idea that these two groups of molecules evolved from a common precursor as first proposed on the basis of sequence comparisons (21). Unlike the mouse Ly-6 proteins, however, CD59 is *N*-glycosylated at N18 (22) and this site is conserved in all known mammalian CD59 sequences except rat CD59 in which the site is shifted by two residues to N16 (23). The contribution of the *N*-glycan to the function of the protein is controversial, however, as its removal or modification has been variously reported to reduce costimulation of proliferation (24), and to eliminate (25), enhance (26), or have no effect on (27, 28) the protective activity of CD59.

To date, no active site of any Ly-6SF molecule has been characterized. The available data are consistent with the proposal that the alpha chain of C8 and the "b" domain of C9 compete for a single binding site on CD59 (29, 30) but the identity of this site is unknown. Ferriani et al. (31) showed that a tryptic fragment of CD59, including disulfide bonded peptides consisting of residues 1–14, 15–30, and 39–41, is able to bind to nascent C5b-8, whereas a study of synthetic peptides by Nakano et al. (32) suggests that the active site is contained within residues 27–38. Kieffer et al. (19) proposed that the non-glycosylated face of CD59 represents a potential ligand binding site because it is relatively hydrophobic and has a series of solvent-exposed phenylalanine and tyrosine residues reminiscent of other sites of protein–protein interaction (33). Consideration of the tertiary structure of CD59, in the context of the analysis of the tryptic fragment by Ferriani et al. (31), led Fletcher et al. (20) to favor residues 20-24 which form a loop on the edge of the domain. Finally, guided by similarities in the rat and human CD59 protein sequences, Rushmere et al. (23) also concluded that the active site could be centred on loop residues 20-24 but drew attention to a conserved hydrophobic pocket lying on the glycosylated face of the extracellular domain between the α-helix and the central β-sheet. In the present study, site-specific mutations of human CD59 have been used to define the regions of the protein required for its complement-inhibitory activity and to examine the role of the glycosylation of the molecule.

Materials and Methods

Genes and Antibodies. Human CD59 cDNA was obtained from Professor Herman Waldmann (Sir William Dunn School of Pathology, Oxford, UK) and Dr. David L. Simmons (Institute of Molecular Medicine, Oxford, UK). The YTH53.1 hybridoma was also obtained from Professor Waldmann. The anti-CD59 monoclonal antibody BRIC 229 was purchased from IBGRL (Elstree, UK); antibody 2/24 was a gift from Dr. A. Fletcher (Australian Red Cross Society, Sydney, NSW, Australia); antibodies MEM43 and MEM43/5 were gifts from Dr V. Horejsi (Czech Academy of Sciences, Prague); antibody A35 was prepared in house (B.P.M., unpublished); antibodies HC1 and HC2 were gifts from Dr. S. Meri (University of Helsinki, Finland). The polyclonal antisera specific for human CD59 and for Chinese hamster ovary (CHO) cell membranes were prepared in house using standard methods.

Mutagenesis and Expression of CD59. A Bam H1 fragment containing the translated region of a CD59 complementary DNA (22) was subcloned into the expression vector pEF-BOS (34). Site-specific mutations were introduced into the gene by in vitro mutagenesis using a commercial kit (Muta-Gene Version 2; Biorad) following the manufacturer's directions. For all mutants, the presence of the desired mutation and fidelity of the part of the gene encoding the rest of the fully processed protein was confirmed by dideoxy sequencing.

Transfection and Expression. CHO cells, in Optimem medium (Life Technologies, Paisley, UK), were transfected with liposomes (Lipofectamine; Life Technologies) containing the expression construct according to the manufacturer's instructions. For analysis of expression levels by FACS®, the cells were detached 48–72 h after transfection, washed three times in FACS® buffer (1% BSA and 0.02% sodium azide in PBS) and resuspended at a density of 5×10^6 cells/ml. The cells were then incubated at 4°C for 30 min with an equal volume (100 μl) of polyclonal anti-human CD59 antibody at 10 μg/ml in FACS® buffer, and then washed three times in FACS® buffer prior to incubation at 4°C for 30 min with FITC-conjugated rabbit anti–mouse IgG at a final concentration of 10 μg/ml in FACS® buffer. Fluorescence of the cells was then analyzed on a FACScan® instrument (Becton Dickinson, Abingdon, Oxford, UK).

Cell Lysis Assay. CHO cells transfected as described above on day 1 were harvested and replated on day 2, and were then left until the plates were confluent (generally day 4). Cells were then washed twice with serum-free medium, incubated in 0.25 ml complete medium (7.5% FCS) containing a 1/750 dilution of calcein-AM (Molecular Probes; 1 mg/ml stock in DMSO) for 1 h at 37°C, then washed once. Triplicate wells were incubated with either medium alone, a 1/5 dilution of normal human serum (NHS) in medium (no FCS), or with a 1/5 dilution of NHS plus blocking antibodies (BRIC 229 and MEM43 both at 10 μg/ml). All wells contained anti-CHO IgG (0.08 μg/ml) in a total volume of 0.25 ml. Blocking antibodies were not complement-fixing and in the absence of anti-CHO did not trigger NHS lysis. After a 1-h incubation at 37°C, all fluid was removed from the cells and transferred to 96-well plates for calcein measurement. The remaining cells were lysed with 0.25 ml PBS containing 0.1% Triton X-100 during a 15-min incubation at room temperature (RT), then the lysate removed to 96-well plates for calcein release assay.

Calcein Release Assay. Calcein fluorescence of supernatants was read in a Denley Wellfluor fluorimeter with the excitation filter set at 485 nm and emission filter at 530 nm. Percent lysis for each well was calculated as specific calcein release/total calcein loading, or:

$$\%\ \text{lysis} = \frac{(\text{NHS calcein release} - \text{background calcein release})}{(\text{NHS calcein release} + \text{detergent calcein release})} \times 100$$

Mean and standard deviations were determined from triplicate samples.

Competition Assay for Anti-CD59 Antibodies. Individual 24-well plates were coated with each of the 8 available antibodies at 10 μg/ml in 0.25-ml aliquots in 25 mM sodium carbonate buffer, pH 9, for 1 h at 37°C. Wells were blocked by incubation in 1% BSA in PBS/0.1% Tween for 1 h at 37°C and washed twice in PBS/Tween, once in PBS alone. Human RBC (0.25 ml of a 1% suspension in PBS), either untreated or preincubated with saturating amounts of each of the antibodies (10 μg/ml, 30 min on ice, followed by two washes in cold PBS), were added to triplicate wells for each coating antibody (and to uncoated, blocked wells as control for nonspecific binding) and incubated at 4°C for 1 h. The wells were washed twice in PBS to remove unbound RBC and then the bound RBC were lysed by addition of water (0.25 ml, 15 min RT). The lysate was removed to a 96-well plate, spun to remove ghosts and the absorbance in the supernatant measured at 412 nm in a plate reader. For each antibody combination, results are expressed as a percentage inhibition derived from the ratio of binding of uncoated RBC/antibody-coated RBC to a particular antibody on the well and are calculated as:

$$\%\ \text{inhibition} = 100 - [\{(\text{Abs1} - \text{Abs2})/(\text{Abs3} - \text{Abs4})\} \times 100],$$

where: Abs1 = absorbance in supernatant from antibody-coated RBC bound to antibody-coated well; Abs2 = absorbance in supernatant from antibody-coated RBC bound to uncoated well; Abs3 = absorbance in supernatant from uncoated RBC bound to antibody-coated well; Abs4 = absorbance in supernatant from uncoated RBC bound to uncoated well. Inhibition was calculated separately for each of the three triplicates and means and standard deviations were determined.

Antibody Binding Assay. CHO cells were transfected with each of the mutant constructs as described above. 2 d after transfection the cells were replated and, after two additional days, detached, and washed twice with serum-free medium then incubated in 0.25 ml complete medium (7.5% FCS) with each of the antibodies (each at approximately 10 μg/ml). Antibody binding to the cells was confirmed by FACS® as described above.

Western Blot. Mutant and wild-type CD59-expressing CHO cells were lysed at 4°C in 1% Triton X-100, 1 μg/ml leupeptin, 1 μg/ml pepstatin A and 1 mM phenlymethylsulphonyl fluoride in PBS. Aliquots of the precleared lysate were electrophoresed in non-reducing buffer in 15% SDS-PAGE gels. The proteins were then electrophoretically transferred to nitrocellulose which was then probed with anti-human CD59 antibody MEM43. Bound antibody was detected using a chemiluminescent detection system (Western-Light, Tropix Inc., Bedford, MA).

Statistical Analysis. Student's *t* test was used to analyze the data.

Results

Mutant Design. Since the region(s) of CD59 responsible for its complement-inhibitory activity are controversial, a systematic mutational analysis of amino acids distributed across the entire surface of the extracellular domain of the protein was undertaken. In using this approach it was assumed that CD59 inhibits MAC formation by binding to another protein, such as C8 or C9. Since the sites of most protein–protein interactions that have been characterized in detail are relatively large (700–900 Å^2) (33) and the surface area of CD59 is small (~3200 Å^2) (19, 20), it seemed likely that the entire surface could be scanned with a small number of mutations. According to this strategy, a first set of mutations was designed to scan both faces and the edges of the disk-like domain at low resolution. Based on the results of the first round of mutagenesis, a second set of mutations was used to analyze specific regions in greater detail.

The selection of particular residues for mutation was based on several criteria. First, only amino acids with side chains pointing away from the structural core of the protein in the NMR structures were chosen. Assuming that the overall conformation of CD59 in the NMR structure represents that of CD59 when bound to a putative ligand

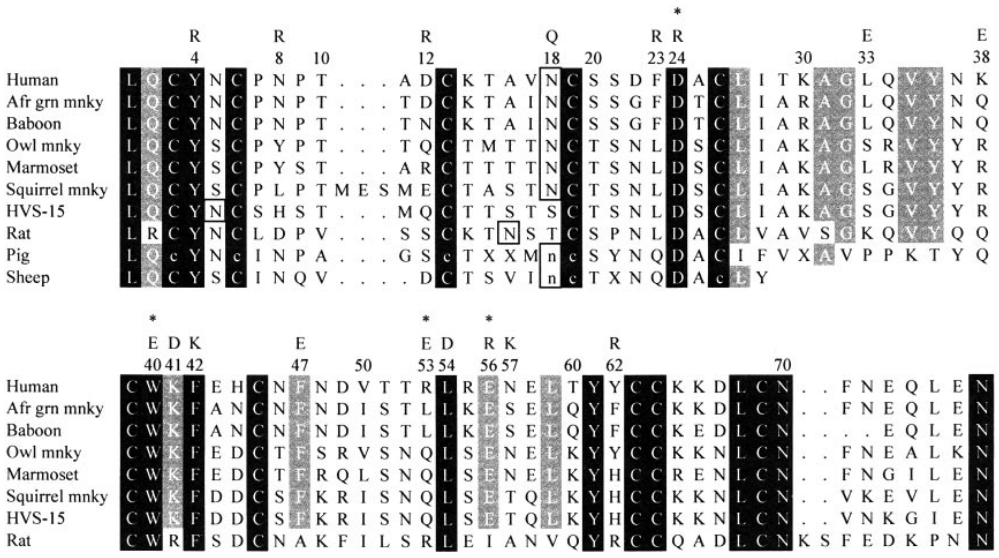

Figure 1. Alignment of CD59 species homologs and HVS-15. Amino acid sequences for the extracellular regions of human (22), African green monkey (11), baboon (11), owl monkey (GenBank accession number: L22861), marmoset (GenBank accession number L22860), squirrel monkey (6), and rat (23) CD59 and Herpesvirus saimiri protein HVS-15 (5) were aligned with the partial sequences of pig (23) and sheep (44) CD59. Residues identical in all sequences are inverse-shaded black and those that are conserved in all species with one exception are inverse-shaded gray. Putative glycosylation sites are boxed. Lower case letters represent probable amino acid assignment, and X represents positions with unknown sequence (23). Residues are numbered according to the sequence of the human mature polypeptide. Every tenth residue is indicated, and both the residue number and introduced substitution are listed for each position selected for mutation. Asterisks mark mutations that disrupted the complement-inhibitory function of human CD59. The sequences were aligned using GCG software (45).

(even though the conformations of the side chains are likely to differ), only side chains of surface residues will directly participate in binding interactions. Second, given the observed lack of strict homologous restriction between certain species (9), it is likely that the active site will include some residues conserved between species so residues representing the most highly conserved of the surface amino acids were selected for mutation (Fig. 1). Third, where possible, mutations were made in regions of the protein implicated in CD59 function by others in order to test their various proposals (19, 20, 23, 31, 32).

Having chosen the sites for mutation, highly nonconservative substitutions were introduced in order to maximize the chances of identifying residues forming the ligand binding surface rather than the smaller subset of residues, identifiable by alanine-scanning mutagenesis, that also contribute significant binding energy to the interaction (35). The likelihood that the mutations would disrupt folding was minimized by confining the substitutions to surface residues. As reasoned previously (36), if a mutant protein is expressed it can generally be expected to have a native-like structure since the drastic changes introduced according to this strategy are unlikely to have subtle effects on the protein fold. The substitutions made in the two rounds of mutagenesis are shown in Fig. 1.

Protective Activity of CD59 Mutants. To facilitate mutant screening, an assay for CD59 function in cells transiently expressing wild-type and mutant CD59 genes was developed. In this assay, transfected cells are loaded with calcein-AM, a fluorescein-based dye that is converted to the fluorescent compound calcein by esterases in live cells. Calcein is effectively retained by intact cells but is released into the medium by lysed cells, where its fluorescence can be measured. The loaded sensitized cells are incubated with normal human serum as a source of complement and the extent of lysis determined by measuring the fluorescence of the released calcein (see Materials and Methods).

The calcein-release assay was used to measure the ability of each of the scanning mutants to inhibit complement-mediated lysis of transiently transfected CHO cells (Fig. 2 *A*). FACS® analysis indicated that the mutant proteins were all expressed at the cell surface at similar levels (Table 1). When the mutant-transfected cells were tested in the calcein-release assay, most were clearly protected from lysis by the presence of the mutant gene when compared with cells transfected with the expression vector alone (Fig. 2 *A*, *black bars*). Consistent with this, co-incubation with CD59-blocking antibodies produced statistically significant reversals of the protective effects of these mutants (Fig. 2 *A*, *white bars*). These results suggest that most of the scanning mutations did not disrupt the folding or the protective activity of CD59. Although mutant F47E provided statistically insignificant protection compared to cells not expressing CD59 ($P = 0.059$), this mutant appeared to have some activity since a significant increase in lysis occurred in the presence of blocking antibodies ($P = 0.004$). Only one of the scanning mutants, W40E, completely failed to provide any protection from complement-mediated lysis. Loss of the inhibitory property of this mutant is not likely to be due to misfolding of the protein since it is recognized by the conformation-sensitive monoclonal antibodies HC1 and MEM43/5 (Table 1). These results indicate that W40 forms at least part of the active site essential for inhibiting the formation of the MAC by CD59. The weak protective effect of the mutant F47E suggests that this residue may be at the periphery of the active site or that it has subtle effects on the conformation of CD59 which indirectly affect its activity.

The sidechain of W40 partially fills a cleft formed by the packing of the α-helix against the three-stranded β-sheet on the glycosylated face of CD59 (19, 20). In a second round of mutagenesis, residues in and around this cleft, specifically K38, K41, R53, L54, and E56, were mutated. Residue D24, which is adjacent to W40 but projects in the opposite direction, was also mutated because it forms part of a conserved loop consisting of residues 20-24 (20, 23). Of these mutants, D24R, R53E, and E56R failed to provide any protection from complement that was reversible by co-incubation with CD59-blocking antibodies (Fig. 2 *B*). All of the mutations that were tested are represented on the NMR structure (19) in Fig. 3, *A–C*.

Antibody Epitopes and Competition Experiments. The binding sites of antibodies that block the complement-inhibi-

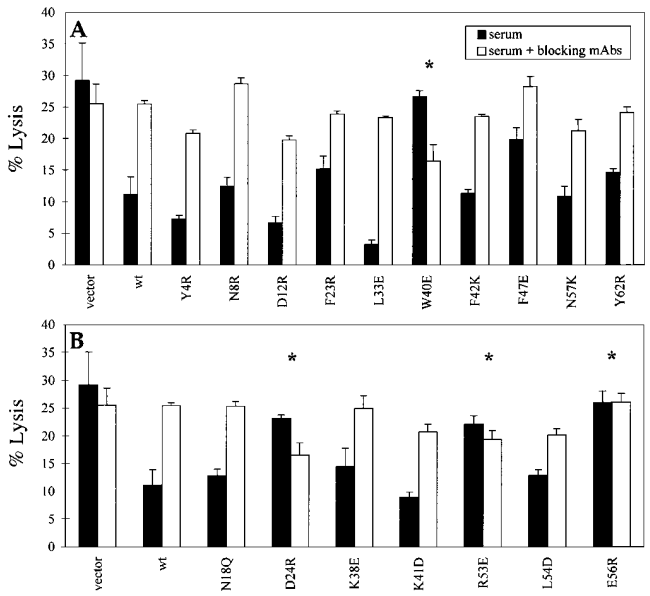

Figure 2. Protection of CD59 mutant-transfected cells from lysis by complement. (*A*) First-round scanning mutations; (*B*) second-round mutations. CHO cells transfected with mutant CD59 genes were loaded with calcein-AM and then subjected to complement attack as described in the Materials and Methods. Percent lysis was calculated from the fluorescence of calcein released by cell lysis as a fraction of total calcein loading as also described in Materials and Methods. For all mutants, the total fluorescence per well was similar to the wild-type value. Mean and standard deviations of % lysis in the presence of NHS alone (*filled bars*) or in the presence of NHS + anti-CD59 blocking antibodies (*open bars*) were calculated from triplicate samples in a single experiment. Asterisks identify mutants which do not protect cells from lysis. Results are from a single experiment; independent replications gave similar results.

Table 1. *Mapping of Anti-CD59 Antibody Epitopes*

	Mutant																		
Antibody	Y4R	N8R	D12R	N18Q	F23R	D24R	L33E	K38E	W40E	K41D	F42K	F47E	R53E	L54D	E56R	N57K	Y62R	Wt	Vector
	% positive																		
Polyclonal	40	35	46	49	42	49	52	30	38	46	44	50	47	50	47	48	44	51	0
BRIC 229	70	71	70	65	66	72	82	52	0	75	69	74	60	62	79	77	75	78	7
YTH 53.1	70	60	68	62	53	64	70	47	16	55	65	74	32	52	74	74	66	77	0
MEM43	82	84	81	80	45	83	89	67	6	45	82	84	17	63	87	87	86	86	0
A35	42	48	49	46	51	60	64	27	5	38	54	54	8	17	35	62	53	58	11
HC2	62	65	61	60	6	74	78	42	0	66	65	68	4	19	54	70	62	68	11
2/24	65	66	65	64	12	70	77	54	0	0	68	72	11	27	67	68	67	68	4
HC1	67	70	62	67	60	73	23	53	44	74	68	72	79	27	6	70	63	72	0
MEM43/5	80	83	76	82	74	84	9	68	61	85	82	84	88	86	83	86	84	87	6
2nd Ab	1	1	1	1	0	1	0	0	1	0	1	1	0	1	0	1	0	1	0

Binding of antibodies to mutant-transfected cells was assessed by FACS® analysis and % positive cells listed. Mutants showing <33% reactivity with a given antibody compared to wild-type cells labeled with the same antibody are shaded black, and mutants with intermediate reactivity (34–52% of wild-type) are shaded gray. Results are from a single experiment; independent replications gave similar results.

tory activity of CD59 are likely to at least partially overlap with the active site of CD59, while epitopes of non-blocking antibodies are expected to lie in a region distinct from the active site. A map of the epitopes of such antibodies can therefore be used to independently confirm the location of the putative active site. A panel of anti-CD59 monoclonal antibodies with differing capacity to block the protective effects of CD59 was selected for this purpose. The panel consists of the antibodies YTH53.1, BRIC 229, MEM43, HC2, and 2/24, which all have strong CD59-blocking activity, A35, which blocks weakly, and HC1 and MEM43/5, which have no CD59-blocking activity (Morgan, B.P., unpublished data).

The antibodies were first characterized in a competition assay (Table 2). Competition between the antibodies was determined by measuring the ability of each antibody, prebound to human RBC, to inhibit the binding of the RBC to plates treated with a second anti-CD59 antibody. Whereas none of the blocking anti-CD59 antibodies competed strongly for binding with the non-blocking antibodies, most pairs of the blocking antibodies were competitive, as observed previously with a subset of these antibodies (37), and consistent with the existence of a single active site on CD59. The only pair of blocking antibodies for which competition was not observed was HC2 and BRIC 229. The possibility that HC2 has relatively weak affinity is suggested by the observation that strong competition for binding sites on HC2-coated RBC only occurred on plates coated with the weakly-blocking antibody, A35.

The antibody epitopes were mapped by measuring the ability of each antibody to bind to CHO cells transfected with each of the mutants. Although this approach cannot delineate their borders precisely, the data show that the epitopes of the blocking antibodies are overlapping but distinct (Table 1 and Fig. 4). All include W40, plus differing portions of continuous surface defined by R53 and other residues adjacent to or in close proximity to W40, suggesting that this region overlaps with the active site of CD59. This is consistent with the results of the calcein-release assay, in which mutants W40E and R53E were unable to protect cells from complement-mediated lysis. It may be significant, however, that mutation of D24 to R did not prevent the binding of any of the blocking antibodies, although this change disrupts CD59 activity. The binding data also indicate that the epitopes of the non-blocking antibodies both lie in a distinct region of the protein which includes L33. However, mutation of E56 to R, which disrupts the function of CD59, also prevents binding of the non-blocking antibody HC1. This implies that the epitope of HC1 and the active site of CD59 partially overlap but in such a way that antibody binding does not completely block CD59 activity. Although the epitope for HC1 appears discontinuous in the figure, this cannot be concluded since the role of intervening residues in antibody binding was not tested.

The Role of Glycosylation. To test the role of the glycans at the highly conserved *N*-glycosylation site in the complement-inhibitory function of CD59, N18 was mutated to

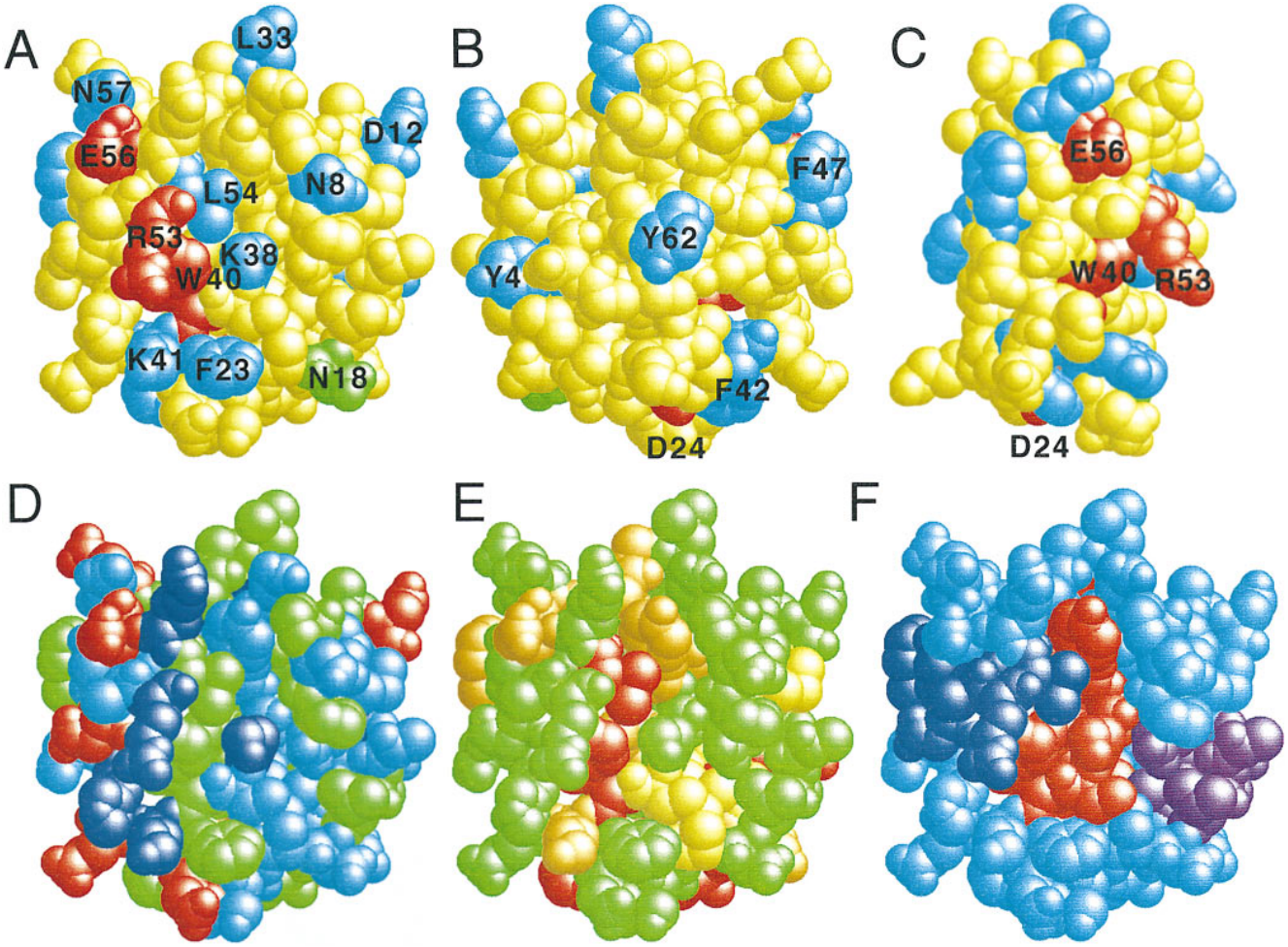

Figure 3. Location and properties of the proposed active site of CD59. (*A–C*) Mutagenesis data. The residues which were mutated are all numbered and those whose mutation reduced protection (* in Fig. 1) or had no effect are colored red and light blue, respectively. N18, which is N-glycosylated, is colored green. Back (*B*) and side (*C*) views differ from the front view (*A*) by 180° and 90°, respectively. (*D*) Chemical features. Hydrophobic residues are colored green, polar uncharged residues, light blue, positively charged residues, dark blue, and negatively charged residues, red. The view is the same as in *A*. (*E*) Conserved residues. Non-cysteine residues that are conserved in all known CD59 sequences and HVS-15 (inverse-shaded black in Fig. 1) are colored red and those conserved in all sequences with one exception (inverse-shaded gray in Fig. 1) are colored orange. Cysteine residues, which are also conserved in all sequences, are colored yellow. The view is the same as in *A*. (*F*) Secondary structure. The positions of the two- and three-stranded β-sheets (*purple* and *red*, respectively) and the α-helix (*dark blue*) of CD59 are shown. Loop residues are colored light blue. The view is the same as in *A*. All of the experimental data are superimposed on the lowest energy NMR structure (19) drawn using Rasmol (46).

Q. The N18Q mutant form of CD59 runs as a single sharp band of ~14 kD on SDS-PAGE, at least 5 kD smaller than wild-type CD59 expressed in CHO cells, which runs as a ladder of bands in the molecular mass range 20–25 kD, and erythrocyte CD59, which runs as a broad smear in the molecular mass range 19–25 kD (Fig. 5). The mobility and banding patterns of all of the other mutants were indistinguishable from those of wild-type CD59 (data not shown). The mobility of N18Q CD59 is similar to that of deglycosylated CD59 (28), indicating that the mutant is not glycosylated. The expression of mutant N18Q at the cell surface, where it binds all of the polyclonal and monoclonal antibodies (Table 1), demonstrates that *N*-glycosylation is not required for native-like folding and expression of human CD59. Mutant N18Q retains wild-type levels of complement-inhibitory activity (Fig. 2 *B*) and binds all of the blocking antibodies at levels similar to that of wild-type CD59 (Table 1), suggesting that the *N*-glycan does not contribute to the active site. This is consistent with the ability of YTH53.1 and BRIC 229 to immunoblot CD59 from endoglycosidase F-treated erythrocytes (37). These data suggest that *N*-glycosylation is not required for the maintenance of the structure or complement-inhibitory function of human CD59.

Discussion

CD59 blocks the complement-mediated lysis of host cells by preventing assembly of the MAC, presumably through binding to C8 and/or C9 molecules in the nascent complex and preventing recruitment of the additional C9 molecules required for pore formation. Whilst it remains for-

Table 2. *Antibody Competition and Blocking Ability*

Plate Antibody	Blocks	RBC Antibody BRIC229	YTH53.1	MEM43	HC2	2/24	A35	HC1	MEM43/5
					% inhibition				
BRIC 229	Yes	88 ± 3	71 ± 5	58 ± 7	21 ± 3	17 ± 3	11± 2	12 ± 5	0 ± 4
YTH 53.1	Yes	79 ± 5	79 ± 7	65 ± 3	40 ± 6	39 ± 6	4 ± 3	2 ± 5	2 ± 3
MEM43	Yes	68 ± 6	49 ± 7	79 ± 3	5 ± 3	62 ± 6	44 ± 3	0 ± 2	12 ± 2
HC2	Yes	15 ± 3	36 ± 5	66 ± 3	78 ± 5	0 ± 1	71 ± 9	11 ± 4	17 ± 4
2/24	Yes	68 ± 5	79 ± 9	85 ± 6	45 ± 2	75 ± 5	88 ± 3	12 ± 4	16 ± 6
A35	Weakly	81 ± 3	72 ± 2	77 ± 5	88 ± 4	15 ± 3	87 ± 5	17 ± 3	8 ± 2
HC1	No	21 ± 4	0 ± 2	8 ± 2	25 ± 3	0 ± 9	40 ± 4	73 ± 6	11 ± 3
MEM43/5	No	13 ± 3	0 ± 6	7 ± 3	12 ± 5	15 ± 3	29 ± 5	17 ± 4	79 ± 5

Antibody-coated RBC were bound to antibody-coated plates and inhibition of binding calculated as described in Materials and Methods. Black shading highlights strong competition (>50% inhibition of binding). Lower levels of inhibition (30–50%), shaded gray, may result from weak competition. Blocking activity is summarized from previously published and unpublished data.

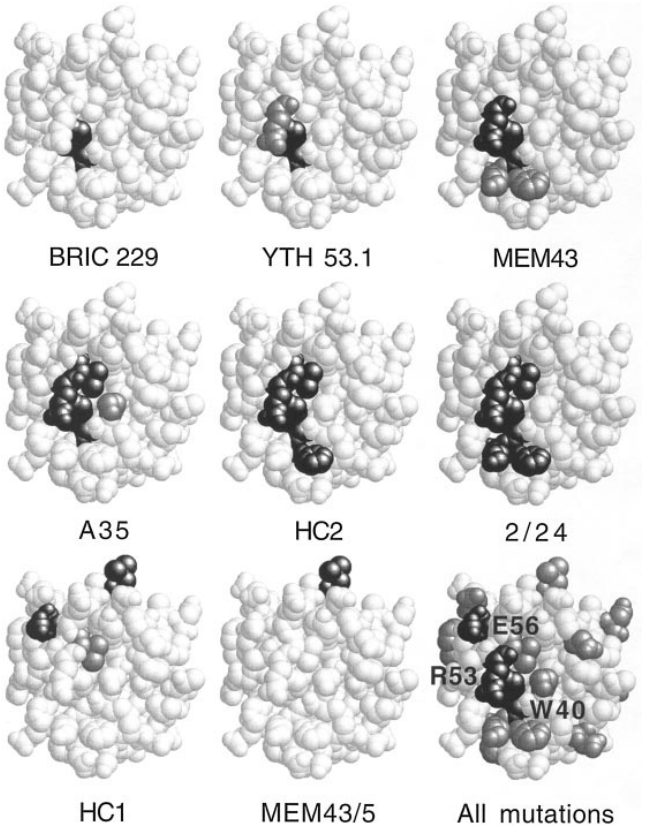

Figure 4. The epitopes of anti-CD59 function-blocking mAb cluster in the region of the proposed active site of CD59. Residues whose mutation disrupted the binding of each antibody (inverse shaded black in Table 1) are shaded black and those whose mutation led to reduced levels of binding (shaded gray in Table 1) are shaded gray. Only antibodies HC1 and MEM43/5 have no CD59-blocking ability. In the last panel, all of the residues that were mutated are shaded gray except for the visible residues whose mutation disrupted the function of CD59 which are shaded black and labeled. In each panel the protein face shown is the one containing the proposed active site shown in the same view as in Fig. 3 *A*. The experimental data are superimposed on the lowest energy NMR structure (19) drawn using Rasmol (46).

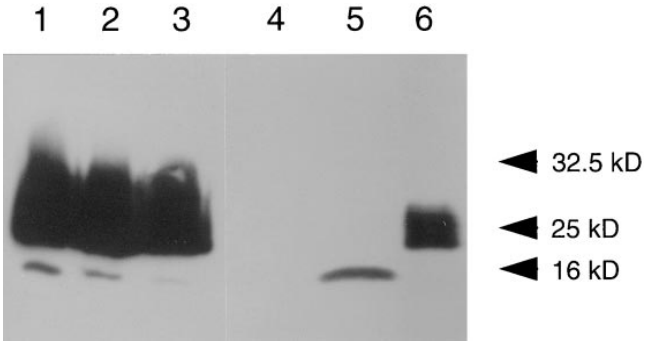

Figure 5. Western-blot analysis of mutant N18Q. CHO cells transfected with the expression vector alone or with the vector expressing wild-type or mutant N18Q CD59 were solubilized and subjected to SDS-PAGE along with purified erythrocyte CD59 and then Western-blotted with anti-CD59 antibody MEM43 as described in the Materials and Methods. Lanes *1*, *2*, and *3* contained 500, 100, and 50 ng of erythrocyte CD59, respectively. Lanes *4*, *5*, and *6* contained aliquots of the cell lysate corresponding to $\sim 5 \times 10^5$ CHO cells transfected with the expression vector alone or with the vector expressing mutant N18Q or wild-type CD59, respectively.

mally possible that CD59 has two distinct binding sites for C8 and C9, the present data strongly suggest that there is a single active site and that this site lies in the vicinity of W40. Mutation of W40 to E eliminates the complement-inhibitory function of CD59 and prevents the binding of all the function blocking anti-CD59 antibodies tested. Although W40 is partially buried in the low resolution NMR structures (19, 20), its mutation to E results in a protein that is probably folded in a predominantly native-like structure

since it is expressed at the cell surface and is recognized by the polyclonal antiserum and both of the non-blocking antibodies to similar extents (60–75% of the wild-type level, Table 1). Mutation of the adjacent residue, R53, which clearly protrudes away from the core of the structure (19, 20), to E also inhibits the complement-inhibitory activity and reduces the binding of four of the six CD59-blocking antibodies, implicating this residue as part of the active site of CD59. A third residue likely to be involved is E56, which lies only 7.5 Å (Cα-Cα) from R53 on the same face of the protein. However, E56 must lie at the periphery of the active site because it constitutes part of the epitope of a non-blocking antibody (Table 1; Fig. 4). Moreover, on the basis of recent carbohydrate analyses of erythrocyte CD59, it has been proposed that, in some tissues, residues T51 and T52, which occupy the region between E56 and R53 but were not mutated in the present study, may be *O*-glycosylated (37a). If this is the case the O-linked glycans are likely to disrupt any contiguous protein surface that includes W40, R53 and E56.

The role of the fourth residue whose mutation disrupted the function of CD59, D24, is less clear as this residue does not form part of a contiguous surface with W40, R53 and E56 (Fig. 3). D24 lies on the edge of the extracellular domain of CD59 only 6 Å from W40 (Cα-Cα; Fig. 3, *A–C*) but is separated from this residue by F23, K41, and F42, all of which were mutated without disrupting the function of the protein. Several explanations could account for this observation. First, it is possible that D24 is part of a discontinuous active site, or that CD59 has a second active site which includes D24. However, both possibilities seem unlikely since none of the epitopes of the panel of six blocking antibodies includes D24. Second, it is conceivable that the mutation of D24 indirectly alters the conformation of key active site residues. However, conformational effects, if these were to occur at all, can only be very restricted given that the D24R mutant binds a series of conformation-sensitive antibodies (Table 1). Finally, the possibility needs to be considered that residue D24, which forms part of a flexible loop (19, 20), is in a sufficiently mobile region of the molecule to allow its direct involvement in forming the active site. Additional experiments are required to determine the role of D24 in the inhibition of complement-mediated lysis.

The affinity of CD59 for the nascent MAC has not been measured directly, although it has been shown that soluble forms of CD59 block the formation of the MAC at relatively low concentrations (~0.5 μM [27]). This suggests that CD59 participates in a protein–protein interaction of relatively high affinity compared to other cell surface protein–protein interactions (38). Sites of protein–protein interaction are often defined by regions of hydrophobic and irregular protein surface (33). In the NMR structures of human CD59 W40 lies at the base of a hydrophobic groove, formed by residues F23, C39, W40, and L54, which is lined on one side by a ridge of hydrophilic residues (K41, H44, R53 and R55; Fig. 3 *D*). Sequence alignments suggest that the hydrophobic groove is among the best conserved regions of CD59 (Fig. 3 *E*) with only F23 exhibiting any variation among the fully sequenced homologues (substitutions to leucine or glutamine; reference 23, Fig. 1). Given the relatively poor overall levels of CD59 sequence conservation and the observed lack of strict homologous restriction between species with known sequences, the conserved hydrophobic groove centred on W40 represents a reasonable candidate for the active site of CD59. Residues 53 and 56, which vary to some extent between species, may contribute some specificity to recognition by CD59. Although mutation of residues F23 and L54, which form part of this hydrophobic groove, did not abrogate the activity of CD59, the putative active site may not have severe topological constraints and, given that these residues are located at the ends of the groove, it is conceivable that the mutants retained sufficient hydrophobic character to be functional.

The NMR analysis of a form of CD59 which includes at least part of the non-lipid component of the GPI-anchor indicated that much of the seven residue COOH-terminal stalk is packed against the non-glycosylated face of the extracellular domain of the molecule (20). This organization of the molecule places the glycosylated face containing the proposed active site in a well exposed, membrane distal position. The NMR study also indicated that in all calculated structures containing model oligosaccharides similar to those present on the protein, the region of the proposed active site remains fully exposed. Consistent with this, the normal expression and full activity of the unglycosylated mutant, N18Q, suggests that the N-linked glycan does not directly contribute to protein folding or complement inhibition by CD59. However, the bulk of the N-linked glycan would be expected to dampen any flexibility at the base of the stalk which could, in turn, keep the extracellular domain in an optimal orientation for interaction with the nascent MAC. Removal of the N-linked glycan could therefore be expected to reduce the affinity of this interaction without eliminating it completely. A partial reduction in the affinity of the N18Q mutant for the MAC could be masked by overexpression of the protein and therefore might have gone undetected in the present study. An indirect role for the N-linked glycan in facilitating the inhibition of complement by CD59 may account for the conservation of the glycosylation site but fails to explain the observation that the enzymatically deglycosylated protein loses most of its activity (25).

The structural analyses of CD59 confirmed that Ly-6SF proteins have topological similarities to snake venom neurotoxins (19, 20). In the crystal structure of a complex between the snake toxin fasciculin and its receptor acetylcholinesterase, the residues that contact the receptor lie on the concave face of the toxin (39). The analogous face is the site of the proposed active site of CD59. Examples of conserved active site locations have been noted previously for other protein–protein recognition molecules including, for example, immunoglobulin superfamily adhesion molecules and cadherins (40, 41). However, the fasciculin-acetylcho-

linesterase crystal structure (39) and functional studies of modified forms of other neurotoxins (42, 43) have revealed that the primary contacts between the toxins and their receptors involve residues of loop II, defined as strands C and D and their connecting loop. In contrast, in CD59, the equivalent loop is significantly shorter and the proposed active site lies instead on the loop between strands D and E on the opposite end of the face. This loop is significantly longer and more elaborate than the corresponding loop in the neurotoxins, which lack the α-helix in this region. These results suggest, not unexpectedly, that the determinants of ligand recognition have diversified considerably since the emergence of protein–protein recognition molecules with this topology.

The authors would like to thank A.N. Barclay for his generous support of the initial stages of these experiments, L.M. Baggott and F.M. Flavin for assistance with sequencing and P.C. Driscoll for providing NMR coordinates of human CD59. D.L. Bodian was supported by the Cancer Research Fund of the Damon Runyon-Walter Winchell Foundation, Fellowship DRG-1246. S.J. Davis, N.K. Rushmere and B.P. Morgan are funded by the Wellcome Trust.

Address correspondence to Simon J. Davis, Molecular Sciences Division, Nuffield Department of Clinical Medicine, Rm 7507, John Radcliffe Hospital, Headington, Oxford OX3 9DU, UK. Dr. Bodian's current address is Bristol-Myers Squibb PRI, 3005 First Avenue, Seattle, WA 98121.

Received for publication 18 June 1996 and in revised form 20 November 1996.

References

1. Ryan, U.S. 1995. Complement inhibitory therapeutics and xenotransplantation. *Nat. Med.* 1:967–968.
2. Brooimans, R., P. van Wieringen, L. van Es, and M.R. Daha. 1992. Relative roles of decay-accelerating factor, membrane cofactor protein, and CD59 in the protection of human endothelial cells against complement-mediated lysis. *Eur. J. Immunol.* 22:3135–3140.
3. Holguin, M.H., L.R. Fredrick, N.J. Bernshaw, L.A. Wilcox, and C.J. Parker. 1989. Isolation and characterization of a membrane protein from normal human erythrocytes that inhibits reactive lysis of the erythrocytes of paroxysmal nocturnal hemoglobinuria. *J. Clin. Invest.* 84:7–17.
4. Yamashina, M., E. Ueda, T. Kinoshita, T. Takami, A. Ojima, H. Ono, H. Tanaka, N. Kondo, T. Orii, N. Okada et al. 1990. Inherited complete deficiency of 20-kilodalton homologous restriction factor (CD59) as a cause of paroxysmal nocturnal hemoglobinuria. *N. Engl. J. Med.* 323:1184–1189.
5. Albrecht, J.-C., J. Nicholas, K.R. Cameron, C. Newman, B. Fleckenstein, and R.W. Honess. 1992. Herpesvirus Saimiri has a gene specifying a homologue of the cellular membrane glycoprotein CD59. *Virology*. 190:527–530.
6. Rother, R.P., S.A. Rollins, W.L. Fodor, J.-C. Albrecht, E. Setter, B. Fleckenstein, and S.P. Squinto. 1994. Inhibition of complement-mediated cytolysis by the terminal complement inhibitor of herpesvirus saimiri. *J. Virol.* 68:730–737.
7. Meri, S., B.P. Morgan, A. Davies, R.H. Daniels, M.G. Olavesen, H. Waldmann, and P.J. Lachmann. 1990. Human protectin (CD59), an 18,000-20,000 MW complement lysis restricting factor, inhibits C5b-8 catalysed insertion of C9 into lipid bilayers. *Immunology*. 71:1–9.
8. Rollins, S.A., and P.J. Sims. 1990. The complement-inhibitory activity of CD59 resides in its capacity to block incorporation of C9 into membrane C5b-9. *J. Immunol.* 144:3478–3483.
9. van den Berg, C.W., and B.P. Morgan. 1994. Complement-inhibiting activities of human CD59 and analogues from rat, sheep, and pig are not homologously restricted. *J. Immunol.* 152:4095–4101.
10. Rollins, S.A., J. Zhao, H. Ninomiya, and P.J. Sims. 1991. Inhibition of homologous complement by CD59 is mediated by a species-selective recognition conferred through binding to C8 within C5b-8 or C9 within C5b-9. *J. Immunol.* 146: 2345–2351.
11. Fodor, W.L., S.A. Rollins, S. Bianco-Caron, W.V. Burton, E.R. Guilmette, R.P. Rother, G.B. Zavoico, and S.P. Squinto. 1995. Primate terminal complement inhibitor homologues of human CD59. *Immunogenetics.* 41:51.
12. Korty, P.E., C. Brando, and E.M. Shevach. 1991. CD59 functions as a signal-transducing molecule for human T cell activation. *J. Immunol.* 146:4092–4098.
13. Hahn, W.C., E. Menu, A.L.M. Bothwell, P.J. Sims, and B.E. Bierer. 1992. Overlapping but nonidentical binding sites on CD2 for CD58 and a second ligand CD59. *Science (Wash. DC).* 256:1805–1807.
14. Deckert, M., J. Kubar, D. Zoccola, C. Bernard-Pomier, P. Angelisova, V. Horejsi, and A. Bernard. 1992. CD59 molecule: a second ligand for CD2 in T cell adhesion. *Eur. J. Immunol.* 22:2943–2947.
15. Arulanandam, A.R.N., P. Moingeon, M.F. Concino, M.A. Recny, K. Kato, H. Yagita, S. Koyasu, and E.L. Reinherz. 1993. A soluble multimeric recombinant CD2 protein identifies CD48 as a low affinity ligand for human CD2: divergence of CD2 ligands during the evolution of humans and mice. *J. Exp. Med.* 177:1439–1450.
16. van der Merwe, P.A., A.N. Barclay, D.W. Mason, E.A. Davies, B.P. Morgan, M. Tone, A.K.C. Krishnam, C. Ianelli, and S.J. Davis. 1994. Human cell-adhesion molecule CD2 binds CD58 (LFA-3) with a very low affinity and an extremely fast dissociation rate but does not bind CD48 or CD59. *Biochemistry*. 33:10149–10160.

17. Williams, A.F. 1991. Emergence of the Ly-6 superfamily of GPI-anchored molecules. *Cell Biol. Int. Rep.* 15:769–777.
18. Ploug, M., and V. Ellis. 1994. Structure-function relationships in the receptor for urokinase-type plasminogen activator. Comparison to other members of the Ly-6 family and snake venom alpha-neurotoxins. *FEBS Lett.* 349:163–168.
19. Kieffer, B., P.C. Driscoll, I.D. Campbell, A.C. Willis, P.A. van der Merwe, and S.J. Davis. 1994. Three-dimensional solution structure of the extracellular region of the complement regulatory protein CD59, a new cell-surface protein domain related to snake venom neurotoxins. *Biochemistry*. 33:4471–4482.
20. Fletcher, C.M., R.A. Harrison, P.J. Lachmann, and D. Neuhaus. 1994. Structure of a soluble, glycosylated form of the human complement regulatory protein CD59. *Structure*. 2: 185–199.
21. Fleming, T., C. O'h Uigin, and T. Malek. 1993. Characterization of two novel Ly-6 genes. Protein sequence and potential structural similarity to alpha-bungarotoxin and other neurotoxins. *J. Immunol.* 150:5379–5390.
22. Davies, A., D. Simmons, G. Hale, R. Harrison, H. Tighe, P. Lachmann, and H. Waldmann. 1989. CD59, an LY-6-like protein expressed in human lymphoid cells, regulates the action of the complement membrane attack complex on homologous cells. *J. Exp. Med.* 170:637–654.
23. Rushmere, N.K., R.A. Harrison, C.W. van den Berg, and B.P. Morgan. 1994. Molecular cloning of the rat analogue of human CD59: structural comparison with human CD59 and identification of a putative active site. *Biochem. J.* 304:595–601.
24. Menu, E., B. Tsai, A. Bothwell, P. Sims, and B. Bierer. 1994. CD59 costimulation of T cell activation. CD58 dependence and requirement for glycosylation. *J. Immunol.* 153:2444–2456.
25. Ninomiya, H., B. Stewart, S. Rollins, J. Zhao, A. Bothwell, and P. Sims. 1992. Contribution of the *N*-linked carbohydrate of erythrocyte antigen CD59 to its complement-inhibitory activity. *J. Biol. Chem.* 267:8404–8410.
26. Akami, T., K. Arakawa, M. Okamoto, K. Akioka, I. Fujiwara, I. Nakai, M. Mitsuo, R. Sawada, M. Naruto, and T. Oka. 1994. Enhancement of the complement regulatory function of CD59 by site-directed mutagenesis at the *N*-glycosylation site. *Transplant. Proc.* 26:1256–1258.
27. Sugita, Y., K. Ito, K. Shiozuka, H. Suzuki, H. Gushima, M. Tomita, and Y. Masuho. 1994. Recombinant soluble CD59 inhibits reactive haemolysis with complement. *Immunology*. 82:34–41.
28. Zhao, J., S.A. Rollins, S.E. Maher, A.L.M. Bothwell, and P.J. Sims. 1991. Amplified gene expression in CD59-transfected Chinese Hamster Ovary cells confers protection against the membrane attack complex of human complement. *J Biol. Chem.* 266:13418–13422.
29. Ninomiya, H., and P.J. Sims. 1992. The human complement regulatory protein CD59 binds to the α-chain of C8 and the "b" domain of C9. *J. Biol. Chem.* 267:13675–13680.
30. Lehto, T., and S. Meri. 1993. Interactions of soluble CD59 with the terminal complement complexes. CD59 and C9 compete for a nascent epitope on C8. *J. Immunol.* 151:4941–4949.
31. Ferriani, V., R. Harrison, and P. Lachmann. 1993. C5b-9 binds to the N-terminal portion of CD59. *Mol. Immunol.* 30(Suppl 1):10.
32. Nakano, Y., T. Tozaki, N. Kikuta, T. Tobe, E. Oda, N.-H. Miura, T. Sakamoto, and M. Tomita. 1995. Determination of the active site of CD59 with synthetic peptides. *Mol. Immunol.* 32:241–247.
33. Janin, J., and C. Chothia. 1990. The structure of protein-protein recognition sites. *J. Biol. Chem.* 265:16027–16030.
34. Mizushima, S., and S. Nagata. 1990. pEF-BOS, a powerful mammalian expression vector. *Nucleic Acids Res.* 18:5322.
35. Cunningham, B.C., and J.A. Wells. 1993. Comparison of a structural and functional epitope. *J. Mol. Biol.* 234:554-563.
36. van der Merwe, P.A., P.N. McNamee, E.A. Davies, A.N. Barclay, and S.J. Davis. 1995. Topology of the CD2-CD48 cell adhesion molecule complex: implications for T cell antigen recognition. *Curr. Biol.* 5:74–84.
37. Fletcher, A., J.A. Bryant, B. Gardner, P.A. Judson, F.A. Spring, S.F. Parsons, G. Mallinson, and D.J. Anstee. 1992. New monoclonal antibodies in CD59: use for the analysis of peripheral blood cells from paroxysmal nocturnal haemoglobinuria (PNH) patients and for the quantitation of CD59 on normal and decay accelerating factor (DAF)-deficient erythrocytes. *Immunology*. 75:507–512.
37a. Rudd, P.M., B.P. Morgan, M.R. Wormald, D.J. Harvey, C.W. van der Berg, S.J. Davis, M.A.J. Ferguson, and R.A. Durk. 1997. Thy glycosylation of the complement regulatory protein, human erythrocyte CD59. *J. Biol. Chem*. In press.
38. van der Merwe, P.A., and A.N. Barclay. 1994. Transient intercellular adhesion: the importance of weak protein-protein interactions. *Trends Biochem. Sci.* 19:354–358.
39. Bourne, Y., P. Taylor, and P. Marchot. 1995. Acetylcholinesterase inhibition by fasciculin: crystal structure of the complex. *Cell.* 83:503–512.
40. Overduin, M., T.S. Harvey, S. Bagby, K.I. Tong, P. Yau, M. Takeichi, and M. Ikura. 1995. Solution structure of the epithelial cadherin domain responsible for selective cell adhesion. *Science (Wash. DC).* 267:386–389.
41. Jones, E.Y., K. Harlos, M.J. Bottomley, R.C. Robinson, P.C. Driscoll, R.M. Edwards, J.M. Clements, T.J. Dudgeon, and D.I. Stuart. 1995. Crystal structure of an integrin-binding fragment of vascular cell adhesion molecule-1 at 1.8 Å resolution. *Nature (Lond.).* 373:539–544.
42. Tremeau, O., C. Lemaire, P. Drevet, S. Pinkasfeld, F. Ducancel, J.C. Boulain, and A. Menez. 1995. Genetic engineering of snake toxins. The functional site of Erabutoxin a, as delineated by site-directed mutagenesis, includes variant residues. *J. Biol. Chem.* 270:9362–9369.
43. Gatineau, E., F. Toma, T. Montenay-Garestier, M. Takechi, P. Fromageot, and A. Menez. 1987. Role of tyrosine and tryptophan residues in the structure-activity relationships of a cardiotoxin from naja nigricollis venom. *Biochemistry*. 26: 8046–8055.
44. van den Berg, C.W., R.A. Harrison, and B.P. Morgan. 1993. The sheep analogue of human CD59: purification and characterization of its complement inhibitory activity. *Immunology*. 78:349–357.
45. Program Manual for the Wisconsin Package, Version 8. 1994. Genetics Computer Group, Madison, WI.
46. Sayle, R.A., and E. Milner-White. 1995. RASMOL: biomolecular graphics for all. *Trends Biochem. Sci.* 20:374.